



# Synthesis and Properties of Symmetrical and Asymmetrical Polyferrocenylmethylenes

Aylin Feuerstein,<sup>[a]</sup> Till Rittner,<sup>[b]</sup> Blandine Boßmann,<sup>[b]</sup> Elias C. J. Gießelmann,<sup>[a]</sup> Justin Schu,<sup>[a]</sup> Bernd Morgenstern,<sup>[a]</sup> Markus Gallei,<sup>\*,[b, c]</sup> and André Schäfer<sup>\*,[a]</sup>

This work is dedicated to Prof. Dr. Ian Manners, acknowledging his pioneering work in the field of metallocene-based polymers.

The synthesis of differently substituted polyferrocenylmethylenes (PFM) via ring-opening transmetalation polymerization (ROTP) is reported. A number of novel, symmetrically and asymmetrically substituted carba[1]magnocenophanes have been prepared, which were used as precursors and allowed investigations of the influence of different substitution patterns on the PFM polymer properties. The novel carba[1]magnocenophanes have been fully characterized by <sup>1</sup>H and <sup>13</sup>C{<sup>1</sup>H} NMR spectroscopy, and structurally authenticated by single-crystal X-ray diffraction (SC-XRD). The corresponding

PFMs were obtained with molecular weights in a range of  $M_w = 1900 \text{ g mol}^{-1}$  up to  $15100 \text{ g mol}^{-1}$  and corresponding dispersities of  $\mathcal{D} = 1.48$  to  $1.81$ . All PFMs have been fully characterized by <sup>1</sup>H and <sup>13</sup>C{<sup>1</sup>H} NMR spectroscopy, as well as by gel permeation chromatography (GPC), thermal gravimetric analysis (TGA) and matrix assisted laser desorption ionization-time-of-flight (MALDI-ToF) mass spectrometry. Pyrolysis of spirocyclic substituted PFM resulted in a ceramic yield above 50%, while the obtained residue was characterized by powder X-ray diffraction (PXRD).

## Introduction

In 1992, the group of Ian Manners laid the foundation for main-chain metallocene-based polymers by introducing the concept of ring-opening polymerization (ROP) of strained sila[1]ferrocenophanes, which gave access to high molecular weight polyferrocenylsilanes (PFS) ( $M_n > 10^5 \text{ g mol}^{-1}$ ).<sup>[1]</sup> Since then, metallocene-based polymers have attracted growing interest due to their outstanding properties as a result of the combination of polymer characteristics with metallocene centers, resulting in a broad series of possible applications, like for example as precursors for nanostructured ceramics, as sensing or smart materials or in biomedical applications.<sup>[2–13]</sup>

Especially ferrocene-based polymers gained broad interest, among other things, due to their thermal and chemical stability, crystallinity, reversible oxidation behavior as well as reactivity as superaromatic electrophile, originating from the ferrocene moieties.<sup>[2,8,14–19]</sup> Through the years, a variety of different bridging motifs have been reported for [1]ferrocenophanes and resulting main-chain ferrocene-based polymers. Beside the iconic sila[1]ferrocenophanes,<sup>[1,2,20,21]</sup> examples for group 13 to 16 element bridged [1]ferrocenophanes are known, with the elements boron,<sup>[22]</sup> aluminium,<sup>[23]</sup> gallium,<sup>[24]</sup> germanium,<sup>[21,25–28]</sup> tin,<sup>[26,29,30]</sup> phosphorous,<sup>[31–35]</sup> sulfur<sup>[36,37]</sup> and selenium.<sup>[36,38–40]</sup> Furthermore, different methods for the ROP of these strained [1]ferrocenophanes have been reported, which include thermal, (living) anionic, photolytic living anionic and the catalytic ROP.<sup>[2,8,31,41–43]</sup> Interestingly, carba[1]ferrocenophanes are unknown, presumably due to their high ring-strain and resulting instability. Thus, no synthetic access for main-chain ferrocene-based polymers with a single carbon atom as bridging motif, “polyferrocenylmethylenes” (PFM), was known until 2021, when the groups of Gallei and Schäfer reported the reaction of symmetrically substituted (dimethyl)carba[1]-magnocenophane with iron(II) bromide to give PFM with molecular weights of  $M_n = 8300 \text{ g mol}^{-1}$  and a polydispersity index of  $\mathcal{D} = 1.40$ .<sup>[40,44]</sup> In recent works, this polymerization reaction type has been referred to as ring-opening transmetalation polymerization (ROTP) as the carba[1]magnocenophane undergoes both a ring-opening and a transmetalation process.<sup>[45]</sup> Unlike in the case of [1]ferrocenophanes, the carba[1] bridging motif in [1]magnocenophanes is known since 1997.<sup>[46]</sup> Compared to ferrocene, where the Fe–Cp bonds exhibit a high covalent character, Mg–Cp bonds possess a much more ionic character,

[a] A. Feuerstein, E. C. J. Gießelmann, J. Schu, B. Morgenstern, A. Schäfer  
*Inorganic Chemistry, Faculty of Natural Sciences and Technology, Department of Chemistry, Saarland University, Campus Saarbrücken, 66123 Saarbrücken, Germany*  
 E-mail: andre.schaefer@uni-saarland.de

[b] T. Rittner, B. Boßmann, M. Gallei  
*Polymer Chemistry, Faculty of Natural Sciences and Technology, Department of Chemistry, Saarland University, Campus Saarbrücken, 66123 Saarbrücken, Germany*  
 E-mail: markus.gallei@uni-saarland.de

[c] M. Gallei  
*Saarland Center for Energy Materials and Sustainability – Saarene, Campus Saarbrücken, 66123 Saarbrücken, Germany*

Supporting information for this article is available on the WWW under <https://doi.org/10.1002/chem.202404283>

© 2024 The Author(s). Chemistry - A European Journal published by Wiley-VCH GmbH. This is an open access article under the terms of the Creative Commons Attribution License, which permits use, distribution and reproduction in any medium, provided the original work is properly cited.

resulting in a more flexible metal-Cp bond and therefore in a decrease of ring strain.<sup>[16,17,47,48]</sup>

In the past, the Manners group demonstrated the influence of the substitution patterns at the bridging atom and at the Cp ring on the polymer properties.<sup>[2,3,49]</sup> In case of PFS systems, they could show a direct correlation between the glass transition temperatures  $T_g$  and the length of the alkyl substituents located at the bridging silicon atom. A decrease of  $T_g$  was observed with an increase in length of the alkyl chains.<sup>[3]</sup> In contrast, substitution of the Cp ring caused a large increase in glass transition temperatures  $T_g$  as well as a loss of crystallinity, and resulted in higher solubility of the polymer in alkane solvents.<sup>[2,49]</sup> In addition, incorporation of functional groups, like for example double bonds, enabling post-polymerization functionalization of the polymer, was demonstrated.<sup>[2,50–53]</sup>

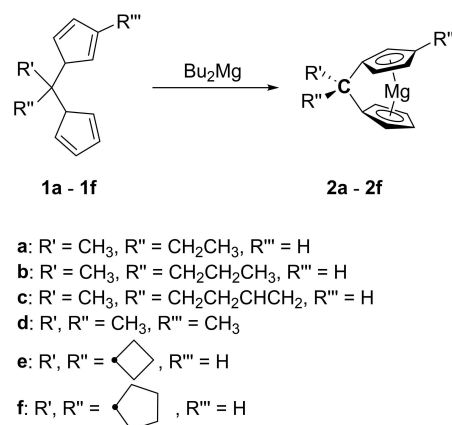
Following our previous report of PFM,<sup>[44]</sup> we have synthesized a number of novel carba[1]magnesocenophanes with various symmetrical and asymmetrical substitution patterns and explored their application as precursors in ROTP, as well as the thermal and solubility properties of the resulting PFM polymers. The investigations also revealed some further insights into the polymerization mechanism of ROTP.

## Results and Discussion

### Carba[1]magnesocenophanes

We started our investigation with the preparation of new carba[1]magnesocenophanes as precursors for the ROTP reactions. Firstly, cyclic and acyclic alkyl groups at the bridging carbon atom with different lengths were introduced, and secondly, a carba[1]magnesocenophane with a methyl substituted Cp ring was synthesized.<sup>[2,49,54,55]</sup> Following the general synthesis route of magnesocenophanes, the neutral *ansa*-ligands 2,2'-bis(cyclopentadienyl)butane **1a**, 2,2'-bis(cyclopentadienyl)pentane **1b**, 2,2'-bis(cyclopentadienyl)hex-5-ene **1c**, 2,2'-(cyclopentadienyl)(methylcyclopentadienyl)propane **1d**, 1,1'-bis(cyclopentadienyl)cyclobutane **1e** and 1,1'-bis(cyclopentadienyl)cyclopentane **1f** were reacted with dibutylmagnesium in hexane (Scheme 1).<sup>[46–48,56,57]</sup> The resulting carba[1]magnesocenophanes **2a–2f** were obtained as highly air-sensitive colorless solids and were characterized by <sup>1</sup>H and <sup>13</sup>C{<sup>1</sup>H} NMR spectroscopy.

In accordance with other carba[1]magnesocenophanes, the <sup>1</sup>H NMR spectra displayed in principle two signal groups, one in the aromatic range for the Cp protons and one high field shifted signal group in the aliphatic range, corresponding to the alkyl moieties. In case of the symmetric substituted **2e** and **2f**, two pseudo triplets are observed at 5.77 ppm and 5.53 ppm for **2e**, respectively 5.71 ppm and 5.54 ppm for **2f**, for the Cp protons in accordance to literature.<sup>[47,48,56]</sup> In contrast, the asymmetric substitution pattern of **2b** and **2c** caused a signal splitting of the Cp protons into four broad signals, respectively seven for **2d**. The two terminal  $sp^2$  carbon atoms of **2c** gave two multiplets in a range of 4.79 ppm to 4.82 ppm and 4.92 to 4.96 ppm. The remaining  $sp^2$  carbon atom is low field shifted in



**Scheme 1.** Synthesis of carba[1]magnesocenophanes **2a–2f** via deprotonation of the neutral *ansa*-ligands **1a–1f** with dibutylmagnesium.

a range of 5.86 to 5.92 ppm. The <sup>13</sup>C{<sup>1</sup>H} NMR spectra are consistent with the <sup>1</sup>H NMR spectra and in accordance with the expected structures of **2a–2f**. Furthermore, **2a–2d** and **2f** could be crystallized in form of their dme-complexes **2a–2d**·dme, **2f**·dme and **2e** in form of its bis(thf)-complex **2e**·(thf)<sub>2</sub>, which allowed for a structural characterization in the solid state by single-crystal X-ray diffraction (SC-XRD) (Figure 1).<sup>[58]</sup> **2a**·dme, **2f**·dme and **2e**·(thf)<sub>2</sub> crystallize in the monoclinic space group  $P2_1/n$ , **2b**·dme and **2c**·dme crystallize both in the monoclinic space group  $P2_1/c$ , while **2d**·dme crystallizes in the orthorhombic space group  $Fddd$ . The fact that **2a–2f** could only be crystallized in form of their donor-solvent adducts is a common phenomenon for Mg–Cp compounds,

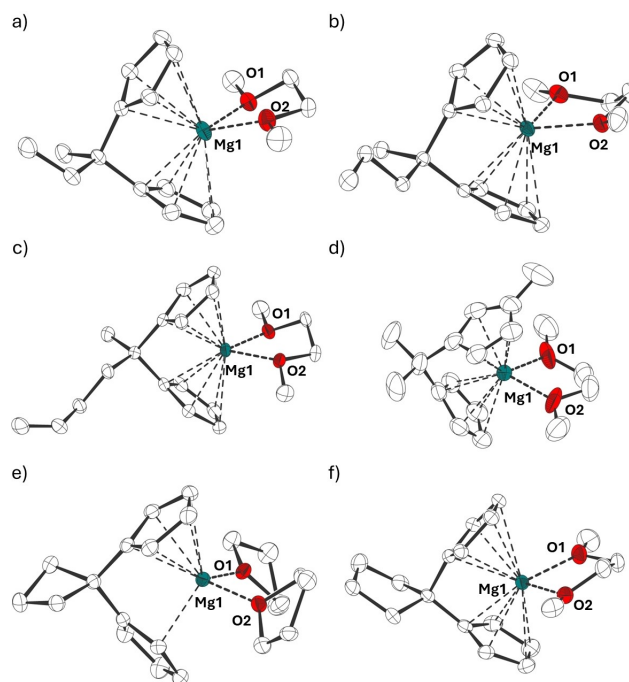


**Figure 1.** Molecular structures in the crystal of a) **2a**·dme, b) **2b**·dme, c) **2c**·dme, d) **2d**·dme, e) **2e**·(thf)<sub>2</sub>, f) **2f**·dme (ellipsoids drawn at 50% probability level, H-atoms omitted for clarity).

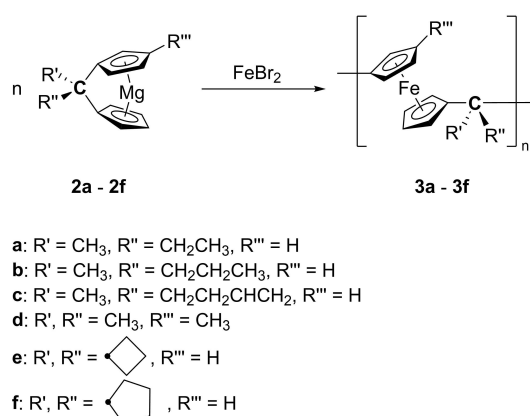
and is a consequence of their very low solubility in non-polar solvents and the Lewis-acidity of the magnesium center.<sup>[47,48,56]</sup>

The solid-state structures of **2a–2d**·dme and **2f**·dme show  $\eta^5/\eta^5$  coordination modes of the Cp rings, which is reported for most magnesocenophane dme adducts (Figure 1).<sup>[47,48,56]</sup> In case of **2e**, the thf coordination causes a ring slippage to an  $\eta^1/\eta^5$  coordination mode. This ring slippage is also a common phenomenon described for several thf adducts of magnesocenophanes.<sup>[47,48,56]</sup> Selected bond lengths and angles of **2a–2d**·, **2f**·dme and **2e**·(thf)<sub>2</sub> are listed in Table 1.

The solid state structures of **2a–2d**·, **2f**·dme and **2e**·(thf)<sub>2</sub> are similar to that of other reported dme and thf complexes, demonstrating that neither the functionalization of the ligands backbone nor a functionalization of the Cp ring has a significant influence on the geometry of the carba[1]-magnesocenophanes.<sup>[47,48,56]</sup>

	Cp hapticity	Mg–Cp <sup>[a,b]</sup> [pm]	Mg–O <sup>[a]</sup> [pm]	$\alpha$ <sup>[c,d]</sup> [deg]	$\delta$ <sup>[c,e]</sup> [deg]
<b>2a</b> ·dme	$\eta^5/\eta^5$	230.33(4); 221.23(4)	204.85(9); 207.26(11)	76.2	119.9
<b>2b</b> ·dme	$\eta^5/\eta^5$	223.21(6); 220.21(5)	209.23(12); 208.04(12)	74.1	120.9
<b>2c</b> ·dme	$\eta^5/\eta^5$	228.08(7); 222.99(6)	205.65(14); 207.42(13)	78.0	121.6
<b>2d</b> ·dme	$\eta^5/\eta^5$	223.66(4);	202.72(13); 206.77(13)	77.9	123.1
<b>2e</b> ·(thf) <sub>2</sub>	$\eta^1/\eta^5$	228.85(12); 212.44(3)	203.77(9); 202.41(9)	–	–
<b>2f</b> ·dme	$\eta^5/\eta^5$	224.07(5); 222.16(4)	206.50(13); 206.72(10)	74.8	120.3

[a] Multiple values are given because the bond is found more than once in the molecule. [b] Corresponding to the bonding mode of the Cp ligand. [c] Only given in case of two  $\eta^5$ -bonded Cp groups. [d] Dihedral angle of  $\eta^5$ -Cp planes. [e] Cp<sup>cent</sup>-Mg-Cp<sup>cent</sup> angle.



**Scheme 2.** Synthesis of polyferrocenylmethylenes **3a–3f** via ring-opening transmetalation polymerization (ROTP) of carba[1]magnesocenophanes **2a–2f**.

## Polyferrocenylmethylenes (PFM)

Carba[1]magnesocenophanes **2a–2f** were reacted with iron(II) bromide in thf at room temperature (Scheme 2). After work-up, the corresponding PFMs **3a–3f** were obtained as orange colored air-stable powders. Analogously to the previously reported PFM and related PFS systems, **3a–3f** were soluble in thf, toluene and chloroform, and demonstrated a hydrophobic character.<sup>[1,2,20,21,44]</sup> It is worth noting that in contrast related polyferrocenylethylenes (PFE) demonstrated lower solubility in common organic solvents.<sup>[59–63]</sup>

Compounds **3a–3f** have been characterized by <sup>1</sup>H and <sup>13</sup>C {<sup>1</sup>H} NMR spectroscopy. In the case of the symmetrically substituted PFMs **3e** and **3f**, two signals for the Cp protons were observed at 4.10 ppm and 3.95 ppm for **3e**, and at 3.95 ppm and 3.84 ppm for **3f**. This is in accordance with the previously reported dimethyl substituted PFM.<sup>[44]</sup> In case of the asymmetric substituted PFMs **3a–3d**, only one broad signal for the Cp protons was observed at 3.91 ppm to 3.90 ppm. For **3d**, a small high field shift for the Cp protons is observed ( $\delta(^1\text{H}) = 3.82$  ppm) due to the inductive effect of the methyl group bound to the Cp ring.<sup>[1,2,20,21,44]</sup>

To determine the molecular weights of PFMs **3a–3f**, gel permeation chromatography (GPC) in thf versus polystyrene standards was performed (Figure S34, supporting information). The molecular weights  $M_n$  and  $M_w$  with the corresponding polydispersity indices  $\mathcal{D}$  are summarized in Table 2. The molecular weights of the asymmetrically substituted compounds **3a–3d** were in the same range as previously reported for poly(ferrocenyldimethylmethylene) ( $M_n = 8300$  g mol<sup>-1</sup>,  $M_w = 11700$  g mol<sup>-1</sup>,  $\mathcal{D} = 1.40$ ).<sup>[44]</sup> However, in case of **3e** and **3f**, only oligomeric species in a range of 1300 and 4900 g mol<sup>-1</sup> could be isolated. One reason might be sterical hindrance of the chain propagation. Another reason could be a result of the symmetric substitution pattern on the bridging carbon atom causing a decrease in solubility of the higher molecular weight polymers. Such a phenomenon was also described in case of the ROP of symmetrically substituted carba[2] systems.<sup>[40,59–63]</sup> In order to increase the molecular weights, different conditions have been varied (temperature, solvent) without success. Likewise, the addition of LiCl or MgBr<sub>2</sub> showed no influence on the molecular weights.<sup>[64–66]</sup>

PFM	$M_n$ <sup>[a]</sup> [g mol <sup>-1</sup> ]	$M_w$ <sup>[a]</sup> [g mol <sup>-1</sup> ]	$\mathcal{D}$
<b>3a</b>	5100	8000	1.56
<b>3b</b>	8000	12100	1.52
<b>3c</b>	9400	15100	1.61
<b>3d</b>	7600	13900	1.81
<b>3e</b>	4900	7500	1.54
<b>3f</b>	1300	1900	1.48

[a] Determined by gel permeation chromatography (GPC) in thf versus polystyrene standards.

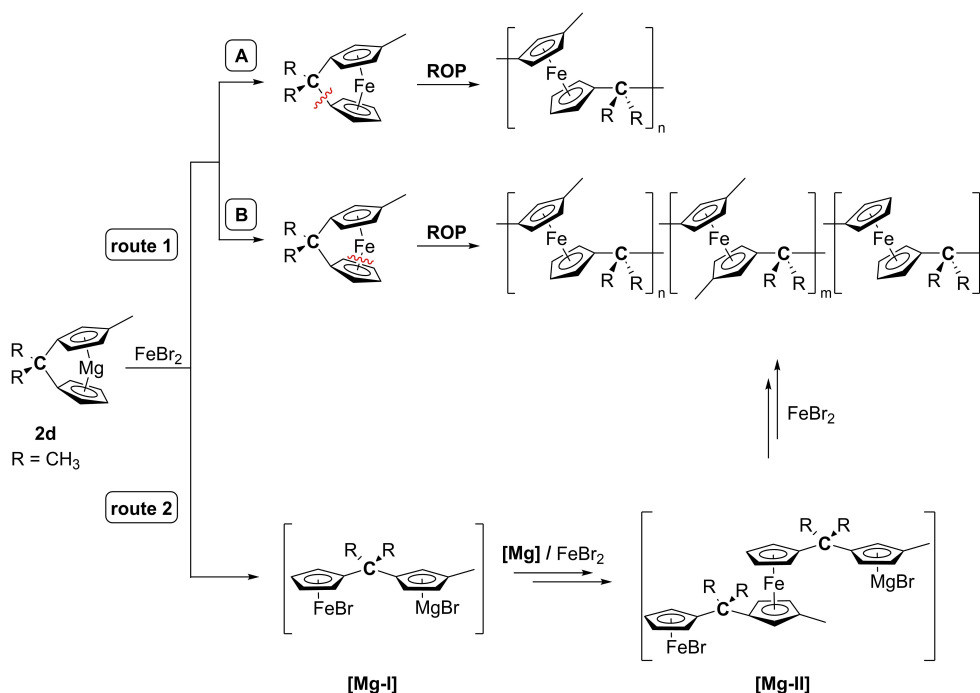
As the mechanism of the ROTP reaction is unclear, MALDI-ToF mass spectrometry measurements of the asymmetrically Cp substituted **3d** were performed to gain some insights into the polymer structure (Figure S35–36, supporting information). In principle, there are two possible polymerization routes (Scheme 3). **Route 1** follows the formation of a carba[1]ferrocenophane, which would most likely undergo instant thermal ROP at room temperature due to its high ring strain. In this case, the thermal ROP could proceed *via* a C–Cp bond cleavage (**route 1-A**), analog to the Si–Cp bond cleavage of sila[1]ferrocenophanes during thermal ROP, or a Fe–Cp bond cleavage (**route 1-B**), analog to the thermal ROP of carba[2]ferrocenophanes.<sup>[54,67]</sup> If the thermal ROP proceeds *via* C–Cp bond cleavage, the polymeric structure of **3d** would only contain one repeat unit, while the Fe–Cp bond cleavage would cause three different repeat units. **Route 2** follows a polycondensation-type reaction. As the carba[1]magnocenophane **2d** can be considered a Grignard-like reagent, formation of the open structure [Mg-I], which can react with further equivalents of FeBr<sub>2</sub> or **2d** to form [Mg-II], respectively PFM, is plausible.

MALDI-ToF mass spectrometry measurements revealed linear and cyclic PFM species analog to the report of poly(ferrocenyldimethyl-methylene).<sup>[44]</sup> The cyclic PFM species are a result of backbiting which was also reported in the thermal ROP of carba[2]ferrocenophanes, where it was postulated to be a result of the heterolytic Fe–Cp bond cleavage, indicating **route 1-B** might be the predominant reaction pathway.<sup>[67]</sup> In addition, a C–Cp bond cleavage (**route 1-A**) would be highly improbable as the C(sp<sup>2</sup>)–C(sp<sup>3</sup>) carbon bonds are expected to be substantially stronger than the Fe–Cp bonds.<sup>[40,67–69]</sup> However, the backbiting could also occur in the Grignard-like intermediates [Mg-I], respectively [Mg-II]. A closer

look at the <sup>13</sup>C{<sup>1</sup>H} NMR spectrum of **3d** reveals various signals for the Cp protons in the range of 101.1 to 102.4 ppm (Figure S20), indicating different ferrocene environments (Cp–Fe–Cp/Cp–Fe–Cp<sup>Me</sup>/Cp<sup>Me</sup>–Fe–Cp<sup>Me</sup>), while there is only one signal for the methylene carbon atom at  $\delta^{13}\text{C}=33.4$  ppm, indicating that the C–Cp bonds stay intact and that there is only a Cp–C–Cp<sup>Me</sup> framework. In sum, a differentiation between **route 1-B** and **route 2** is not possible on the basis of the MALDI-ToF and <sup>13</sup>C{<sup>1</sup>H} NMR data, but **route 1-A** can most likely be ruled out. The molecular weights obtained for **3d** are significantly lower than the ones reported for thermal ROP of sila[1]ferrocenophanes and carba[2]ferrocenophanes ( $M_n \approx 10^5 \text{ g mol}^{-1}$ ), which, in combination with the fact that we could not observe or isolate a carba[1]ferrocenophane even at low temperatures, strongly suggests that the ROTP of **2d** follows **route 2** and is a polycondensation-type reaction involving Grignard-like intermediates.<sup>[1,36,40,59]</sup>

As metal-containing polymers can be used as preceramic materials, we were interested to study the thermal behavior of **3a–3f** by thermogravimetric analysis (TGA) and differential scanning calorimetry (DSC).<sup>[44,70–72]</sup> The corresponding TGA curves under a nitrogen atmosphere in a temperature range of 30 to 600 °C, as well as the DSC thermograms are given in Figure S32 and S33 in the supporting information. The observed glass transition temperatures  $T_g$  and the corresponding ceramic yields are summarized in Table 3.

Similarly to poly(ferrocenyldimethylmethylene), for **3a–3d** and **3f**, degradation starts at around 110 °C, while a distinct weight loss is observed at around 350 °C up to 460 °C for **3a**, up to 430 °C for **3b**, up to 400 °C for **3c** and up to 390 °C for **3d**.<sup>[44]</sup> Only in case of **3e**, degradation takes place in three steps from 100 °C to 180 °C, the second up to 380 °C and the last one up to



**Scheme 3.** Overview of possible reaction routes of the ring-opening transmetalation polymerization (ROTP) of **2d** with FeBr<sub>2</sub>.

**Table 3.** Glass transition temperatures  $T_g$  and ceramic yields of **3a–3e**.

PFM	Ceramic yield (N <sub>2</sub> ) [wt%]	$T_g$ [°C]
<b>3a</b>	29.2	100.4
<b>3b</b>	24.3	105.1
<b>3c</b>	43.5	87.0
<b>3d</b>	17.6	94.2
<b>3e</b>	51.0	62.0
<b>3f</b>	28.9	95.7

520 °C. After the treatment under nitrogen, the samples turned into a black material, exhibiting macroscopic ferromagnetic properties.

As mentioned above, the Manners group had already reported a strong influence of the substitution pattern in PFS systems on the polymers  $T_g$  and we had demonstrated that substitution of the silicon atom by a carbon atom has a profound impact on the  $T_g$ . For instance, the symmetrically dimethyl-substituted PFM system exhibits a  $T_g$  of 60.5 °C, which is well above the  $T_g$  reported for the analogues PFS system (33 °C).<sup>[13,44]</sup> This is explained by the more rigid nature of the Cp–C–Cp bond compared to the Cp–Si–Cp bond. In case of PFS, an increase of the alkyl chain length leads to a decrease in  $T_g$ .<sup>[3]</sup> This is however not observed for the PFM systems **3a–3f**, which exhibit  $T_g$ s of 62.0 to 105.1 °C. Interestingly, **3e** has by far the lowest  $T_g$  of this series, but also a remarkably high ceramic yield of 51% compared to other linear ferrocene-containing polymers.<sup>[44,55,73–76]</sup> Similarly, **3c** shows the second lowest  $T_g$  along with the second highest ceramic yield, which could be a result of cross-linking due to the double bond in the polymers backbone, respectively the four membered ring system. Due to the high ceramic yield of **3e**, further investigations have been performed by elemental analysis of **3e** and powder X-ray diffraction (PXRD) of its pyrolysis residue (Figure S31, supporting information). The elemental analysis of **3e** revealed 69.33% carbon and 5.76% hydrogen, which is in a good agreement with the calculated values (C: 70.62%, H: 5.93%). The PXRD pattern of the ceramic obtained by pyrolysis revealed a mainly amorphous compound with nanocrystalline domains of elemental iron, further explaining the powders ferromagnetic behavior. However, the poor quality of the PXRD data obtained is a result of the residue's low crystallinity.

## Conclusions

In conclusion, we synthesized novel symmetrically and asymmetrically substituted carba[1]magnocenophanes, which were fully characterized by <sup>1</sup>H and <sup>13</sup>C{<sup>1</sup>H} spectroscopy, as well as SC-XRD. Furthermore, they were applied as precursors in ROTP reactions with iron(II) bromide. The obtained PFM polymers have been fully characterized by <sup>1</sup>H and <sup>13</sup>C{<sup>1</sup>H} NMR spectroscopy, as well as GPC, TGA and DSC measurements. The polymers'  $T_g$  values are much higher than what has been

reported before for analogues silicon systems (PFS) and the introduction of groups enabling cross-linking caused a substantial increase of the ceramic yields, of up to 51%. Investigations into the underlying reaction mechanism of ROTP suggest a polycondensation-type reaction of a Grignard-like reagent. Furthermore, a C=C double bond moiety was introduced in the backbone, which might allow post-functionalization of the PFM polymer in future work.

## Acknowledgements

The authors thank Dr. Alexander Schießer (Department of Chemistry, Mass Spectrometry, Technische Universität Darmstadt) for the MALDI-ToF mass spectrometry measurements (INST 163/445-1 FUGG). Susanne Harling is thanked for elemental analysis. Open Access funding enabled and organized by Projekt DEAL.

## Conflict of Interests

The authors declare no conflict of interest.

## Data Availability Statement

The data that support the findings of this study are available in the supplementary material of this article.

**Keywords:** Polyferrocenylmethylenes • Polymerization • Metallopolymers • Magnesocenophane • Iron

- [1] D. A. Foucher, B.-Z. Tang, I. Manners, *J. Am. Chem. Soc.* **1992**, *114*, 6246–6248.
- [2] R. L. N. Hailes, A. M. Oliver, J. Gwyther, G. R. Whittell, I. Manners, *Chem. Soc. Rev.* **2016**, *45*, 5358–5407.
- [3] K. Kulbaba, I. Manners, *Macromol. Rapid Commun.* **2001**, *22*, 711–724.
- [4] a) X. Wang, H. Wang, D. J. Frankowski, P. G. Lam, P. M. Welch, M. A. Winnik, J. Hartmann, I. Manners, R. J. Spontak, *Adv. Mater.* **2007**, *19*, 2279–2285; b) D. J. Frankowski, J. Ræz, I. Manners, M. A. Winnik, S. A. Khan, R. J. Spontak, *Langmuir* **2004**, *20*, 9304–9314; c) K. Temple, K. Kulbaba, I. Power-Billard, K. N. Manners, K. A. Leach, T. Xu, T. P. Russell, C. J. Hawker, *Adv. Mater.* **2003**, *15*, 297–300.
- [5] Y. Yan, J. Zhang, L. Rend, C. Tang, *Chem. Soc. Rev.* **2016**, *45*, 5232–5263.
- [6] S. Basak, A. Bandyopadhyay, *J. Organomet. Chem.* **2021**, *956*, 122129.
- [7] J. Zhou, G. R. Whittell, I. Manners, *Macromolecules* **2014**, *47*, 3529–3543.
- [8] V. Bellas, M. Rehahn, *Angew. Chem. Int. Ed.* **2007**, *46*, 5082–5104.
- [9] C. Rüttiger, H. Hübner, S. Schöttner, T. Winter, G. Cherkashinin, B. Kuttich, B. Stühn, M. Gallei, *ACS Appl. Mater. Interfaces* **2018**, *10*, 4018–4030.
- [10] R. Pietschnig, *Chem. Soc. Rev.* **2016**, *45*, 5216–5231.
- [11] Y. Gao, J. M. Shreeve, *J. Inorg. Organomet. Polym. Mater.* **2007**, *17*, 19–36.
- [12] A. S. Abd-El-Aziz, I. Manners, *J. Inorg. Organomet. Polym. Mater.* **2005**, *15*, 157–195.
- [13] A. Schäfer, in *Comprehensive Organometallic Chemistry IV, Vol. 14* (Eds.: G. Parkin, K. Meyer, D. O'hare), Elsevier, **2022**, 3–22.
- [14] J. Rasburn, R. Petersen, T. Jahr, R. Rulkens, I. Manners, G. J. Vancso, *Chem. Mater.* **1995**, *7*, 871–877.
- [15] T. Chuard, R. Deschenaux, *Chimia* **1998**, *52*, 547.
- [16] K. E. Lewis, G. P. Smith, *J. Am. Chem. Soc.* **1984**, *106*, 4650–4651.

- [17] Y. Sha, Y. Zhang, E. Xu, Z. Wang, T. Zhu, S. L. Craig, C. Tang, *ACS Macro Lett.* **2018**, *7*, 1174–1179.
- [18] D. Astruc, *Eur. J. Inorg. Chem.* **2017**, *2017*, 6–29.
- [19] a) C. G. Hardy, L. Ren, J. Zhang, C. Tang, *Isr. J. Chem.* **2012**, *52*, 230–245; b) C. G. Hardy, J. Zhang, Y. Yan, L. Ren, C. Tang, *Prog. Polym. Sci.* **2014**, *39*, 1742–1796.
- [20] I. Manners, *Polyhedron* **1996**, *15*, 4311–4329.
- [21] N. P. Reddy, H. Yamashita, M. Tanaka, *J. Chem. Soc., Chem. Commun.* **1995**, 2263–2264.
- [22] H. Braunschweig, R. Dirk, M. Müller, P. Nguyen, R. Resendes, D. P. Gates, I. Manners, *Angew. Chem.* **1997**, *109*, 2433–2435.
- [23] J. A. Schachner, C. L. Lund, J. W. Quail, J. Müller, *Organometallics* **2005**, *24*, 785–787.
- [24] B. Bagh, J. B. Gilroy, A. Staubitz, J. Müller, *J. Am. Chem. Soc.* **2010**, *132*, 1794–1795.
- [25] D. A. Foucher, M. Edwards, R. A. Burrow, A. J. Lough, I. Manners, *Organometallics* **1994**, *13*, 4959–4966.
- [26] F. Jäkle, R. Rulkens, G. Zech, J. A. Massey, I. Manners, *J. Am. Chem. Soc.* **2000**, *122*, 4231–4232.
- [27] S. Zürcher, V. Gramlich, A. Togni, *Inorg. Chim. Acta* **1999**, *291*, 355–364.
- [28] N. S. Jeong, I. Manners, *Macromol. Chem. Phys.* **2009**, *210*, 1080–1086.
- [29] F. Jäkle, R. Rulkens, G. Zech, D. A. Foucher, A. J. Lough, I. Manners, *Chem. Eur. J.* **1998**, *4*, 2117–2128.
- [30] R. Rulkens, A. J. Lough, I. Manners, *Angew. Chem. Int. Ed.* **1996**, *35*, 1805–1807.
- [31] T. Mizuta, Y. Imamura, K. Miyoshi, *J. Am. Chem. Soc.* **2003**, *125*, 2068–2069.
- [32] T. J. Peckham, A. J. Lough, I. Manners, *Organometallics* **1999**, *18*, 1030–1040.
- [33] T. Mizuta, M. Onishi, K. Miyoshi, *Organometallics* **2000**, *19*, 5005–5009.
- [34] E. K. Sarbisheh, J. C. Green, J. Müller, *Organometallics* **2014**, *33*, 3508–3513.
- [35] C. H. Honeyman, D. A. Foucher, F. Y. Dahmen, R. Rulkens, A. J. Lough, I. Manners, *Organometallics* **1995**, *14*, 5503–5512.
- [36] R. Rulkens, D. P. Gates, D. Balaishis, J. K. Pudelski, D. F. McIntosh, A. J. Lough, I. Manners, *J. Am. Chem. Soc.* **1997**, *119*, 10976–10986.
- [37] J. K. Pudelski, D. P. Gates, R. Rulkens, A. J. Lough, I. Manners, *Angew. Chem.* **1995**, *107*, 1633–1635.
- [38] I. Manners, *Adv. Organomet. Chem.* **1995**, *37*, 131–168.
- [39] H. Bhattacharjee, J. Müller, *Coord. Chem. Rev.* **2016**, *314*, 114–133.
- [40] D. E. Herbert, U. F. J. Mayer, I. Manners, *Angew. Chem. Int. Ed.* **2007**, *46*, 5060–5081.
- [41] U. F. J. Mayer, J. B. Gilroy, D. O'Hare, I. Manners, *J. Am. Chem. Soc.* **2009**, *131*, 10382–10383.
- [42] J.-J. Wang, L. Wang, X.-J. Wang, T. Chen, H.-J. Yu, W. Wang, C.-L. Wang, *Mater. Lett.* **2006**, *60*, 1416–1419.
- [43] M. Tanabe, I. Manners, *J. Am. Chem. Soc.* **2004**, *126*, 11434–11435.
- [44] T. Winter, W. Haider, A. Schießer, V. Presser, M. Gallei, A. Schäfer, *Macromol. Rapid Commun.* **2021**, *42*, 2000738.
- [45] A. Feuerstein, B. Boßmann, T. Rittner, R. Leiner, O. Janka, M. Gallei, A. Schäfer, *ACS Macro Lett.* **2023**, *12*, 1019–1024.
- [46] C. Cremer, H. Jacobsen, P. Burger, *Chimia* **1997**, *51*, 650–653.
- [47] L. Wirtz, A. Schäfer, *Chem. A Eur. J.* **2021**, *27*, 1219–1230.
- [48] L. Wirtz, W. Haider, V. Huch, M. Zimmer, A. Schäfer, *Chem. A Eur. J.* **2020**, *26*, 6176–6184.
- [49] A. Presa Soto, L. Chabanne, J. Zhou, J. B. Gilroy, I. Manners, *Macromol. Rapid Commun.* **2012**, *33*, 592–596.
- [50] L. Chabanne, S. Pfirrmann, D. J. Lunn, I. Manners, *Polym. Chem.* **2013**, *4*, 2353–2360.
- [51] D. J. Lunn, C. E. Boott, K. E. Bass, T. A. Shuttleworth, N. G. McCreanor, S. Papadouli, I. Manners, *Macromol. Chem. Phys.* **2013**, *214*, 2813–2820.
- [52] W. Y. Chan, A. Y. Cheng, S. B. Clendinning, I. Manners, *Macromol. Symp.* **2004**, *209*, 163–176.
- [53] F. Wurm, S. Hilf, H. Frey, *Chem. A Eur. J.* **2009**, *15*, 9068–9077.
- [54] J. K. Pudelski, I. Manners, *J. Am. Chem. Soc.* **1995**, *117*, 7265–7266.
- [55] M. J. MacLachlan, A. J. Lough, I. Manners, *Macromolecules* **1996**, *29*, 8562–8564.
- [56] L. Wirtz, J. Lambert, B. Morgenstern, A. Schäfer, *Organometallics* **2021**, *40*, 2108–2117.
- [57] P. Perrotin, P. J. Shapiro, M. Williams, B. Twamley, *Organometallics* **2007**, *26*, 1823–1826.
- [58] Deposition numbers 2403055 (for **2a** dme), 2403057 (for **2b** dme), 2403054 (for **2c** dme), 2403056 (for **2d** dme), 2403051 (**2e** (thf)<sub>2</sub>), 2403052 (for **2f** dme) contain the supplementary crystallographic data for this paper. These data are provided free of charge by the joint Cambridge Crystallographic Data Centre and Fachinformationszentrum Karlsruhe Access Structures service.
- [59] J. M. Nelson, P. Nguyen, R. Petersen, H. Rengel, P. M. Macdonald, A. J. Lough, I. Manners, D. O'Hare, *Chem. Eur. J.* **1997**, *3*, 573–584.
- [60] D. E. Herbert, U. F. J. Mayer, J. B. Gilroy, M. J. López-Gómez, A. J. Lough, J. P. H. Charmant, I. Manners, *Chem. Eur. J.* **2009**, *15*, 12234–12246.
- [61] J. M. Nelson, H. Rengel, I. Manners, *J. Am. Chem. Soc.* **1993**, *115*, 7035–7036.
- [62] G. Masson, A. J. Lough, I. Manners, *Macromolecules* **2008**, *41*, 539–547.
- [63] R. W. Heo, F. B. Somoza, T. R. Lee, *J. Am. Chem. Soc.* **1998**, *120*, 1621–1622.
- [64] C. Kloninger, M. Rehahn, *Macromolecules* **2004**, *37*, 1720–1727.
- [65] H. Wang, M. A. Winnik, I. Manners, *Macromolecules* **2007**, *40*, 3784–3789.
- [66] D. E. Herbert, J. B. Gilroy, Y. C. Wing, L. Chabanne, A. Staubitz, A. J. Lough, I. Manners, *J. Am. Chem. Soc.* **2009**, *131*, 14958–14968.
- [67] J. B. Gilroy, A. D. Russell, A. J. Stonor, L. Chabanne, S. Baljak, Mairi F. Haddow, I. Manners, *Chem. Sci.* **2012**, *3*, 830–841.
- [68] M. B. Smith, J. March, *Advanced Organic Chemistry*, John Wiley & Sons, New York, **2001**.
- [69] H. J. Bernstein, *J. Chem. Soc., Faraday Trans.* **1962**, *58*, 2285–2306.
- [70] C. Rüttiger, V. Pfeifer, V. Rittscher, D. Stock, D. Scheid, S. Vowinkel, F. Roth, H. Didzoleit, B. Stühn, J. Elbert, E. Ionescu, M. Gallei, *Polym. Chem.* **2016**, *7*, 1129–1137.
- [71] D. Scheid, G. Cherkashinin, E. Ionescu, M. Gallei, *Langmuir* **2014**, *30*, 1204–1209.
- [72] G. Mera, M. Gallei, S. Bernard, E. Ionescu, *Nanomaterials (Basel)* **2015**, *5*, 468–540.
- [73] M. A. Hempenius, C. Cirmi, F. Lo Savio, J. Song, G. J. Vancso, *Macromol. Rapid Commun.* **2010**, *31*, 772–783.
- [74] A. G. Osborne, R. H. J. Whiteley, *Organomet. Chem.* **1975**, *101*, C27.
- [75] A. G. Osborne, R. H. Whiteley, R. E. J. Meads, *Organomet. Chem.* **1980**, *193*, 345.
- [76] R. Petersen, D. A. Foucher, B.-Z. Tang, A. Lough, N. P. Raju, J. E. Greedan, I. Manners, *Chem. Mater.* **1995**, *7*, 2045–2053.
- [77] G. R. Fulmer, A. J. M. Miller, N. H. Sherden, H. E. Gottlieb, A. Nudelman, B. M. Stoltz, J. E. Bercaw, K. I. Goldberg, *Organometallics* **2010**, *29*, 2176–2179.
- [78] G. M. Sheldrick, *Acta Cryst.* **2015**, *A71*, 3–8.
- [79] G. M. Sheldrick, *Acta Cryst.* **2015**, *C71*, 3–8.
- [80] C. B. Hübschle, G. M. Sheldrick, B. Dittrich, *J. Appl. Crystallogr.* **2011**, *44*, 1281–1284.
- [81] *Topas (version 5)*; Bruker AXS Inc.: Karlsruhe (Germany), **2014**.
- [82] I. E. Nifant'ev, V. L. Yamykh, M. V. Borzov, B. A. Mazurchik, V. I. Mstyslavsky, V. A. Roznyatovsky, Y. A. Ustyniyuk, *Organometallics* **1991**, *10*, 3739–3745.
- [83] B. Wang, B. Mu, X. Deng, H. Cui, S. Xu, X. Zhou, F. Zou, Y. Li, L. Yang, Y. Li, Y. Hu, *Chem. A Eur. J.* **2005**, *11*, 669–679.
- [84] L. Sha, L. Li, F. Yuan, *Chin. J. Chem.* **2014**, *32*, 1214–1216.
- [85] J. Paradies, G. Erker, R. Fröhlich, *Angew. Chem. Int. Ed.* **2006**, *45*, 3079–3082.

Manuscript received: November 21, 2024  
Accepted manuscript online: December 23, 2024  
Version of record online: January 15, 2025